

Communication

# Post-Lithium Batteries with Zinc for the Energy Transition

Julia Pross-Brakhage <sup>1,\*</sup>, Oliver Fitz <sup>2</sup> , Christian Bischoff <sup>2</sup>, Daniel Biro <sup>2</sup>  and Kai Peter Birke <sup>1</sup> 

<sup>1</sup> Institute for Photovoltaics, Electrical Energy Storage Systems, University of Stuttgart, 70569 Stuttgart, Germany

<sup>2</sup> Fraunhofer Institute for Solar Energy Systems ISE Battery Cell Technology, Department of Electrical Energy Storage, 79110 Freiburg, Germany

\* Correspondence: julia.pross-brakhage.2@ipv.uni-stuttgart.de

**Abstract:** The energy transition is only feasible by using household or large photovoltaic powerplants. However, efficient use of photovoltaic power independently of other energy sources can only be accomplished employing batteries. The ever-growing demand for the stationary storage of volatile renewable energy poses new challenges in terms of cost, resource availability and safety. The development of Lithium-Ion Batteries (LIB) has been tremendously pushed by the mobile phone industry and the current need for high-voltage traction batteries. This path of global success is primarily based on its high energy density. Due to changing requirements, other aspects come to the fore that require a rebalancing of different technologies in the “Battery Ecosystem”. In this paper we discuss the evolution of zinc and manganese dioxide-based aqueous battery technologies and identify why recent findings in the field of the reaction mechanism and the electrolyte make rechargeable Zn-MnO<sub>2</sub> batteries (ZMB), commonly known as so-called Zinc-Ion batteries (ZIB), competitive for stationary applications. Finally, a perspective on current challenges for practical application and concepts for future research is provided. This work is intended to classify the current state of research on ZMB and to highlight the further potential on its way to the market within the “Battery Ecosystem”, discussing key parameters such as safety, cost, cycle life, energy and power density, material abundance, sustainability, modelling and cell/module development.



**Citation:** Pross-Brakhage, J.; Fitz, O.; Bischoff, C.; Biro, D.; Birke, K.P. Post-Lithium Batteries with Zinc for the Energy Transition. *Batteries* **2023**, *9*, 367. <https://doi.org/10.3390/batteries9070367>

Academic Editor: Junnan Hao

Received: 24 April 2023

Revised: 13 May 2023

Accepted: 27 June 2023

Published: 8 July 2023



**Copyright:** © 2023 by the authors. Licensee MDPI, Basel, Switzerland. This article is an open access article distributed under the terms and conditions of the Creative Commons Attribution (CC BY) license (<https://creativecommons.org/licenses/by/4.0/>).

## 1. Introduction

In 2019 the Nobel prize for chemistry was awarded for the development of the LIB technology. This technology exhibits a tremendous advantage. The intercalation electrodes, where ions can be precisely placed on lattice vacancies of the electrode, host materials [1]. The principle can be compared to a sponge, where water can be taken up and released thousands of times. What the sponge does on a macroscopic scale is performed in LIB electrodes on a microscopic scale. Consequently, the batteries can be manufactured in the discharged state, which has many advantages in production. Additionally, the intercalation electrodes lead to distinctly higher lifetime cycle expectations and energy density over other battery technologies such as lead-acid [2]. In the end, this is the overriding technical reason for LIB ruling the automotive market for high-voltage traction batteries. However, this only becomes feasible in connection with battery-pack costs of USD 100 per kWh<sup>-1</sup> which are foreseen in 2023 [3]. Regarding the current prices for stationary battery storage systems, the reality is still quite different, as one can purchase 20 kWh for about USD 10.000 to 24.000 [4] for household storage applications employing photovoltaic modules together with batteries. This raises the question of how such stationary applications can be tackled. Since photovoltaic and wind-based power plants are very volatile, storage systems such as batteries are indispensable if pursuing 100% renewable energy. Tesla has built a 129 MWh

LIB in Australia, one of the largest in the world [5]. However, this is supported by a local-grid business model which is quite specific for the geographical prerequisite in Australia. We can easily deduce that, rather than USD 10 per kWh<sup>-1</sup> per pack, USD 100 per kWh<sup>-1</sup> are required to serve multiple stationary applications by batteries and thereby make the energy transition feasible. One idea is to put LIB from automotive applications into a second life. Since stationary applications usually require lower power demands vs. automotive applications and batteries can be kept at ideal temperatures, this idea basically makes sense. One could resell such a battery for about USD 10–30 per kWh<sup>-1</sup> and the business model behind it would be feasible. However, these batteries will come back from the market in large numbers in about 10 years at the earliest. No one really knows yet about the Weibull distribution, which means that failures could accumulate after a certain lifetime exponentially. Additionally, the cycle behaviour is quite confirmed up to 70% initial capacity, but few data are available for less than that. Additionally, the LIB chemistry is still under development. Therefore, many batteries in different formats with different chemistries will emerge. Although standardization is a highly important issue, it is not present yet. This leads to the conclusion that the need of alternative battery technologies is exceedingly high. Since the last decades of battery development were ruled by energy density, people were focusing less on alternative developments. In recent years, the development of a promising battery technology has undergone a silent revolution. A system commonly known as alkaline manganese, correctly zinc–manganese dioxide, is becoming rechargeable through new electrolyte approaches. This system has the potential to address the cost issue towards the order of magnitude of USD 10 per kWh<sup>-1</sup> on pack level and promises advantages in terms of safety, abundancy and environmental compatibility. In this paper, we reveal the underlying chemistry, present first results and discuss the new battery technology within the ecosystem of stationary batteries and energy transition.

## 2. History and Development of Aqueous Zinc–Manganese Dioxide Batteries

Batteries based on the material combination of zinc and manganese dioxide have a long history of development and commercialization, which at the same time provides important insights for understanding the underlying mechanisms and challenges. As the research field is huge and developing fast, we will not try to cover every aspect of the development of ZMB but try to reflect important milestones in particular, which are shown in Figure 1.

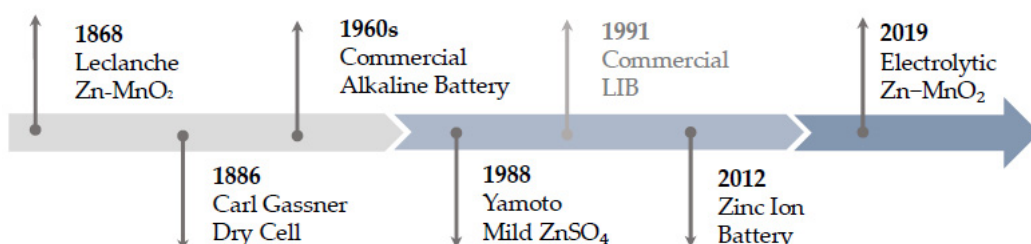


**Figure 1.** Timeline development of zinc and manganese dioxide-based battery technologies.

The first of its kind and forerunner of all generations was the Leclanche cell, also known as the “wet” Leclanche cell, which was invented by Georges Leclanche in 1868 and uses mild acid ammonium chloride as an electrolyte [6]. The concept of the dry counterpart, which was less susceptible to leakage and enabled transportation [7], is based on jellified ammonium and zinc chloride and was patented by Carl Gassner in 1886. However, the corrosion of the zinc anode in combination with ammonium chloride still leads to comparatively short service lives.

For that reason, they were subsequently displaced by the development and commercialization of the alkaline manganese cell in the 1960s [8]. Here, the electrolyte was replaced by an alkaline electrolyte consisting of potassium hydroxide. The principle of operation for the first-generation ZMB is shown in Figure 2. At the anode, the zinc undergoes a dissolu-

tion process and dissolves in the solution as zincate, whereas at the cathode manganese dioxide is converted through a solid-state conversion to MnOOH. The biggest hurdle in the application of the technology for large-scale grid storage is the poor cycling performance related to the formation of irreversible products at the cathode and passivation processes and restructuring of the active material at the anode, which is why this technology is used exclusively as a primary battery [9].

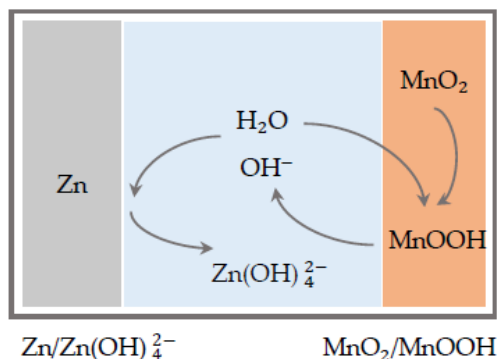


**Figure 2.** Function mechanisms of first-generation alkaline ZMB.

In 1986, Yamamoto introduced a technology with a slightly acidic electrolyte with zinc sulphate, which was supposed to improve the rechargeability, but received little attention nevertheless [10]. This may be because this was at a time when LIB technology had reached marketability and Sony had launched the first commercially available cell in 1991 [11]. The first to revisit this approach were Xu et al. in 2012, who used a moderately acidic  $\text{ZnSO}_4$  electrolyte in  $\alpha\text{-MnO}_2$  that exhibited good reversibility and cyclability [12]. Here, the intercalation of zinc ions into the cathode is proposed as the reaction mechanism for the first time. By analogy to the rocking chair principle of the LIB, the term zinc-ion battery is established and heralds the start of a proximate generation and strong increase in research interest [12–32].

While the first publications concentrate on phase transition and the crystallographic structure of  $\text{MnO}_2$  [18,33,34], Lee and colleagues were the first to describe the critical role of the pH value on the reaction mechanism [35]. They demonstrated that the pH is subject to fluctuations during cyclization associated with the dissolution of  $\text{MnO}_2$  and, as a result, zinc hydroxide sulphate (ZHS) precipitates in the electrolyte [36–38].

This is confirmed by the study of Bischoff et al., which shows local pH changes in the electrolyte by adding a pH indicator to the electrolyte solution [39]. Since that time, the underlying storage mechanism has been under controversial debate. Pan et al. are the first to propose reversible intercalation of hydrogen ions as a reaction mechanism and prove this by showing that the performance drops dramatically in anhydrous organic solvents [40]. Furthermore, to reduce the dissolution of the cathode, additional manganese sulphate is added to the electrolyte, resulting in much longer cycle life. Sun et al. link these concepts and show two characteristic regions in the discharge curve, which they assign first to zinc intercalation and second to hydrogen insertion [21]. The mechanisms for the second-generation ZMB are shown schematically in Figure 3. Moreover, a capacity of  $290 \text{ mAh g}^{-1}$  ( $0.3 \text{ C}$ ) is reached, which is close to the theoretical capacity of  $\text{MnO}_2$  based on molecular weight and if one-electron reaction via  $\text{Mn}^{4+}/\text{Mn}^{3+}$  redox couple for  $\text{Zn}^{2+}$  or  $\text{H}^+$  insertion/extraction mechanism is assumed ( $308 \text{ mAh g}^{-1}$ ). This is also within the range of capacities that could be achieved in related concepts [18,22,23].

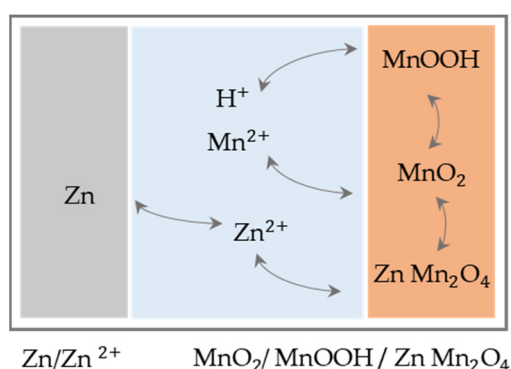


**Figure 3.** Function mechanisms of second-generation ZMB with mild acid aqueous electrolyte.

Chao's group also assigns the potential domains to the underlying reaction mechanisms, identifying an additional mechanism in the upper potential range between 1.7–2.0 V that is assigned to the electrolytic deposition and dissolution of manganese dioxide which can be forced in a targeted manner by adding sulfuric acid [41]. This theory has been supported by Li et al. and Guo et al., who also already point out the importance of improving the capacity of the electrolyte to absorb excess OH<sup>-</sup>, but without talking directly about buffer substances [36,42]. The studies of Fitz et al. [43] prove the periodic pH changes triggered by pH-relevant ions such as OH<sup>-</sup> and H<sup>+</sup> and quantify them by in-operando pH tracking during cycling. The pH changes during the operation can be assigned to the different reaction mechanisms mentioned in the literature so far and emphasize the major contribution of the MnO<sub>2</sub> deposition mechanism. In addition, the finding of the importance of the MnO<sub>2</sub> electrolytic deposition is supported by the publication of Li et al., which even questions the Zn<sup>2+</sup> intercalation mechanism [37]. A summary of the reported reaction mechanism in literature based on [43] can be found in the Supplementary Materials Table S1 [44–54].

Considering the achieved capacity of 570 mAh g<sup>-1</sup> (1 C) by Chao et al. [41], which is almost doubled, the big leap forward in technology becomes clear and argues for the start of another cell generation based on a novel mechanism with two-electron Mn<sup>4+</sup>/Mn<sup>2+</sup> reaction, pictured in Figure 4 for the third-generation ZMB. The nominal voltage reported here is 1.95 V, which is significantly higher than the voltage plateau of about 1.3 V otherwise observed with zinc-ion batteries [55]. This is attractive because the energy density increases linearly with the usable voltage, which can thus be significantly increased.

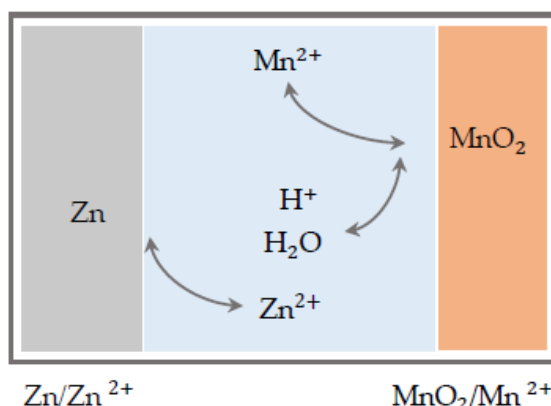


**Figure 4.** Function mechanisms of third-generation electrolytic ZMB.

At the same time, it is generally accepted that the stability of the zinc anode against hydrogen evolution and corrosion decreases significantly in the acidic pH range (<pH 4) [56]. One approach to deal with this problem is to decouple the electrolyte environment of the respective electrodes. To prevent mixing, however, the electrolyte must be demobilized for this purpose, which can be achieved, for example, by jellification or ion-selective mem-

brates. While the latter is associated with high costs, jellification leads to significantly higher overvoltage and therefore lower performance [57,58].

A different approach is taken by Mateos et al., who demonstrate that the two-electron mechanism can be accessible even under mild non-corrosive conditions by creating a local proton environment through the addition of buffer substances [59]. In addition, it turns out that the type of anion has a strong effect on the pH value and the solvation structure, which forces the desired deposition mechanism [60,61]. This was the starting point for a rapidly evolving research field of electrolyte engineering, which will be discussed in Section 4 in more detail.

In summary, the latest generation of zinc and manganese-based systems are promising in terms of longevity and achievable energy density compared to previous generations. The next section will now discuss the strengths and challenges of the technology and answer the question of how this technology should be classified in the battery ecosystem.

### 3. Zinc–Manganese Batteries in the Context of Battery Ecosystem

Battery development undergoes a paradigm change. While just few years ago, only energy density, power density, cycle/calendar life, safety and costs were ruling all business, now raw material supply, environmental sustainability, social criteria, upcycling, recycling and digitalization are added. The enlargement process of this so called “Battery ecosystem” necessitates a rebalancing of the technologies, which is shown schematically in Figure 5a. In the future, this ecosystem will become of huge importance for all kinds of battery technologies. Thus, we will see a diversification, and the dominance of LIB will be relativized to some extent in the coming years.

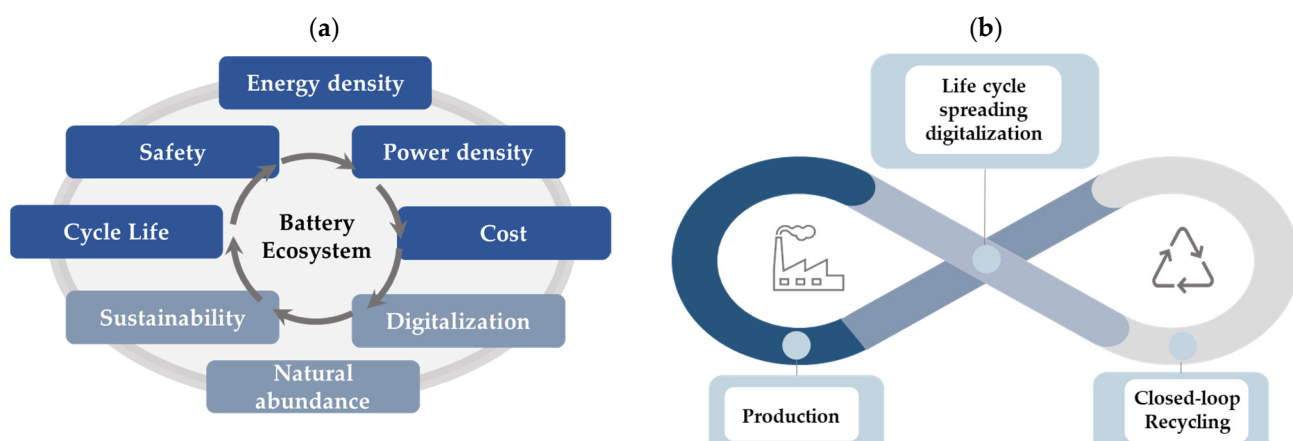


**Figure 5.** (a) Rebalancing of battery technologies with respect of the transformation from “Battery ecosystem”. (b) Life cycle spreading digitalization.

Although ZMB may not be the first choice for high energy-density-demanding automotive applications, these batteries are urgently required for stationary demands and can play a pivotal role in this ecosystem, which we will discuss in the following.

#### 3.1. Digitalization

Digitalization in production is urgently required to reduce scrap. Producing 1 billion battery cells per year, which is usual in GWh factories, means having 10% scrap: 100 million cells are waste. Digitalization in the sense of gathering data within the single production steps and using this data to improve quality and to identify waste before assembling it to a complete cell will be the key enabler to reduce waste and to push cell quality. The latter is urgently needed if plenty of cells are assembled in serial connections. Digitalization over the entire life cycle of batteries is shown in Figure 5b.

### 3.2. Safety

Renewable energy requires a very safe and reliable storage solution, and safety should be seen as a prerequisite for any advanced electrochemical energy storage technology. The biggest challenge in this respect for LIBs is the usage of flammable organic electrolytes. This is circumvented in ZMB systems by using aqueous electrolytes that are not combustible. In addition, because water has five times higher heat capacity than a conventional solvent for LIBs, ZAB can tolerate greater overall temperature fluctuations [62].

At the same time, hydrogen evolution at the negative electrode must also be mentioned as probably the most important factor in terms of the safety of aqueous batteries [63]. Here, experience with lead-acid batteries can be drawn upon, and simultaneously considerable research effort has demonstrated that the reduction of hydrogen evolution can be achieved by measures such as adding electrolyte additives and applying electrode coatings, which are discussed in more detail in Section 4.

### 3.3. Cost

A cost estimate for a new technology presents a major challenge. This is particularly evident in the continuing rapid price development of LIBs in recent decades, which is illustrated in Figure 6a. In the year 2000, the cost per kilowatt hour of a LIB pack was eighteen times the current price and there are estimates that costs will fall even further by 2030 [3], based on the assumptions that material prices will continue to decrease and that the production rate and energy density will increase.

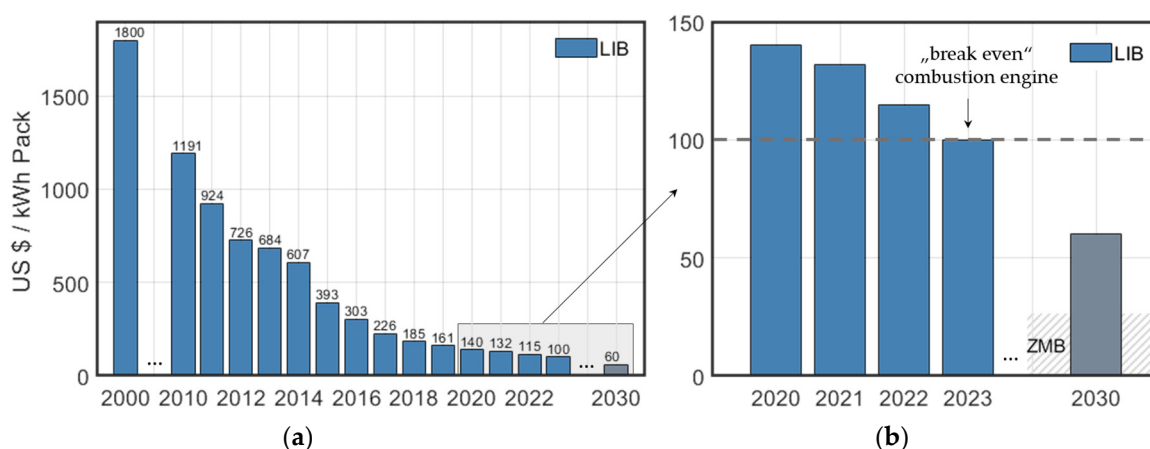


**Figure 6.** Development of cost for (a) LIB packs between 2000 and 2030 and (b) certain part of LIB zoomed in between 2020 and 2030 and prognosis for price trend for ZMB. In order to illustrate that it is difficult to make statements about price developments, the costs for the year 2030 are deliberately shown in grey.

Even though almost every publication emphasizes the low cost of ZMB, there are only a few publications that make a specific statement about it. The first to give an estimate of the cost of active materials are Chao et al. who arrive at a value of about USD 5 per  $\text{kWh}^{-1}$  [41], which is in a similar order of magnitude to what we calculated in our own estimates (Supplementary Materials Table S2). Although the cost of the active materials, normalized to the storables energy, is a good starting point for bottom-up analyses, it should be emphasized that the level of battery scale (material/cell/module/pack/systeminstalled system level) is a crucial factor that is often not clearly identified in many studies. Song et al. go a step further and look at the costs of ZAB and LIB in comparison based on the BatPac 4.0 simulation tool [64]. Assuming a two-electron transfer mechanism and anode utilization of 90%, they calculate costs of USD 18 per  $\text{kWh}^{-1}$  at the material level (including passive material) and USD 45 per  $\text{kWh}^{-1}$  at the pack level, which includes costs for materials, processing, labour and capital equipment. However, the authors also point out that the

cost structure of LIB has simply been adopted here, although large differences in terms of production can be observed.

Expensive dry-room processing, which is required to produce conventional LIBs and critical solvents such as NMP, which are harmful to health and costly to recover, can be dispensed with [65]. In particular, this means that the manufacturing process is significantly simplified and the investment costs for setting up a production plant will be significantly lower. Additionally, there is the possibility of being able to completely forego with the costly production of electrode coatings and to significantly simplify the process by direct deposition during the first charging process. Finally, it may be possible to revert to a simplified pack architecture due to the lower demand on the cooling and monitoring system. It can therefore be assumed that a completely different cost structure must be expected here, and new approaches must first be determined in further studies.

Since the basic components of these batteries are similar to the frequently used disposable alkaline batteries, the costs of less than USD 20 per kWh<sup>-1</sup> for this technology can be used for validation [66], with the cost of active materials being USD 9 per kWh<sup>-1</sup> [67]. Sporerke et al. present a practical roadmap for low-cost battery manufacturing of rechargeable alkaline batteries and shows that USD 50 per kWh<sup>-1</sup> can realistically be achieved [68]. Here it is worth emphasizing, again, that the decisive factor is the access to usable capacity, which in alkaline batteries is currently only 20% of the one-electron mechanism [69] and illustrates the great potential of using the two-electron mechanism again, which is discussed in detail in Section 2.

The current sharp rise in electricity prices makes it clear that a consideration of the economic viability is only reliable for a very limited period of time, and a holistic techno-economic evaluation would also go beyond the scope of our study. Nevertheless, with a fair degree of certainty one can say that ZAB is the cheaper alternative to LIB and is suitable for stationary energy storage based on current calculations. The development of many start-ups on the basis of this technology emphasizes the attractiveness and indicates the enormous potential [70–73]. A short summary can be found in Supplementary Materials Table S5 [74–80].

### 3.4. Cycle Life

Regarding the cycle stability, the literature shows full cell results for ZMB cells in a large scattering range of, e.g., 30 to 10,000 cycles, whereby high cycle numbers of 2000–3000 cycles with a residual capacity of well over 80% are often mentioned [81–83]. Figure 7b shows published Coulomb efficiencies over cycle life for selected publications that use buffer additives in the electrolyte. Here it is clear that a high level of capacity retention can be obtained over the lifetime, which speaks for a high reversibility. Nevertheless, a meaningful indication of the cycle stability due to the still debated reaction mechanism and other influences such as the different cycling parameters (charge/discharge currents in the range of, e.g., 0.1 mA g<sup>-1</sup> up to 6,160 mA g<sup>-1</sup>, the latter corresponding to the equivalent of approx. 20 C [25,82–85]), of the different mass loadings of the cathode (e.g., in the range of 15 mg cm<sup>-2</sup> to approx. 10 mg cm<sup>-2</sup> [83,84,86]) and the different cell structures (e.g., coin cells, Swagelok® cells, El-Cells®, in-house developments) is hardly possible. As shown in Table 1, the proof-of-concept with application-oriented mass loadings of the electrodes, C-rates in the range of application-oriented numbers, e.g., for stationary applications (C-rates < 1 C) and application-oriented cell formats still needs to be done. This will become clearer during further research on this battery cell chemistry with the evaluation of application-oriented cell structures in the future.

**Table 1.** Overview of the cell composition and the mass loadings of the electrodes, the electrolyte composition and its initial pH value, the cell format, the C-rate and the initial capacity as well as the cycle stability for selected publications with pH-buffered electrolytes. For C-rate calculations, see Supplementary Materials Calculations S3.

Cell Composition (Mass Loading)		Electrolyte Composition (Initial pH)	Cell Format	Initial Capacity (C-Rate)	Source
Anode	Cathode				
zinc foil	MnO <sub>2</sub> , acetylene black, PVDF on carbon paper (1.5–8 mg cm <sup>-2</sup> )	1 M ZnSO <sub>4</sub> , 0.1 M MnSO <sub>4</sub> , 25 mM NHP-buffer (pH ~ 2.8)	coin cells (CR2032)	~100 mAh g <sup>-1</sup> , equal to ~0.4 mAh cm <sup>-2</sup> (~10 C)	[83]
zinc foil	carbon-cloth (“cathode-free”)	1 M ZnSO <sub>4</sub> , 1 M MnSO <sub>4</sub> , 0.2 M CH <sub>3</sub> COOH (pH~2)	pouch cell (2.25 cm <sup>2</sup> )	0.8 mAh cm <sup>-2</sup> (12.5 C)	[83]
zinc foil	MnO <sub>2</sub> -coated GLAD-ITO (~30 µg cm <sup>-2</sup> )	0.25 M ZnCl <sub>2</sub> , 0.1 M MnCl <sub>2</sub> , 1.5 M CH <sub>3</sub> COOH (pH~5)	spectro-electrochemical cell	~100 mC cm <sup>-2</sup> , equal to ~0.03 mAh cm <sup>-2</sup> (~36 C)	[86]
zinc foil	MnO <sub>2</sub> , carbon black, PVDF on carbon fibre sheet (10 mg cm <sup>-2</sup> )	2 M ZnSO <sub>4</sub> , 1 M C <sub>4</sub> H <sub>6</sub> O <sub>6</sub> (pH ~ 4)	not specified	7000 mA g <sup>-1</sup> , 374 mAh g <sup>-1</sup> , (~18.7 C)	[86]

Furthermore, as shown in the course of this paper, the electrolyte composition has a significant influence on the reaction mechanism of the ZMB regarding the initial pH value and the pH changes during cycling [35–37,39,43], the Zn<sup>2+</sup>/Mn<sup>2+</sup> salts and their concentration [87] and electrolyte additives such as pH buffering substances [36,42,59,83,86,88,89].

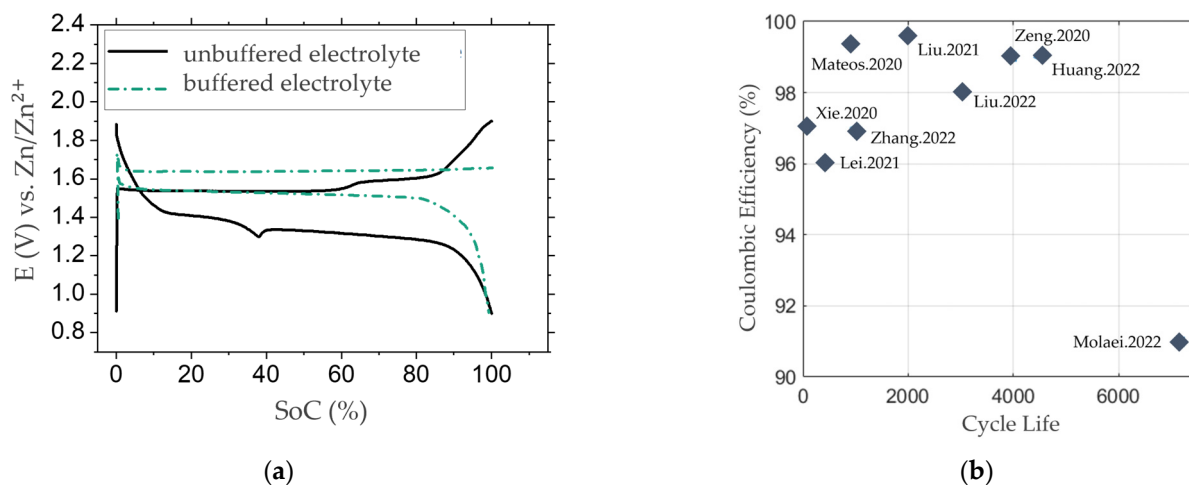


**Figure 7.** (a) Comparison of the typical potential curves of ZMB with either pH-unbuffered (based on [39]) or pH-buffered electrolytes (based on [86]). There is a more stable potential plateau visible for pH-buffered electrolytes due to the reduction of pH changes during operation of the cell. (b) Overview over the cycle life of selected publications with buffered electrolytes, showing high Coulomb efficiencies as an indicator for good capacity retention [60,61,83,86,88–92].

In Figure 7, typical potential curves for selected ZMB publications with either pH-unbuffered [39] and pH-buffered [86] (pH buffer capability of the electrolyte by the addition of acetic acid) electrolytes are compared. For the unbuffered electrolyte, the typical potential bend during discharge at 1.3 V vs. Zn/Zn<sup>2+</sup> is visible, compared to the more stable potential behaviour during operation of the buffered electrolyte. Regarding Mateos et al. [86], this

performance is explained by the reduction of pH changes during operation of the ZMB with pH-buffered electrolytes, as the pH-dependent Nernst equation shows. For showing cycle stability graphs of ZMB, the focus is set on selected publications with pH-buffered electrolytes to represent the current status of ZMB research (Table 1).

### 3.5. Energy Density

To estimate the energy density potential and thus the influences on the specific costs of the ZMB technology, an exemplary calculation of the amount of electrolyte can be carried out. This estimation is viable insofar as the electrolyte represents the energy storage reservoir in the form of the dissolved  $Zn^{2+}$  and  $Mn^{2+}$  ions by one of the suggested reaction mechanisms (e.g.,  $Mn^{2+}/MnO_2$  deposition/dissolution). This scales the amount of electrolyte with the storable energy in the battery. Based on estimating calculations, the volumetric and gravimetric energy density can therefore be calculated on the basis of the necessary amount of electrolyte (without electrode materials, passive materials and other peripheral materials) using Faraday's law and certain assumptions for ZMB electrolytes (Supplementary Materials Table S2):

- gravimetric energy density approx.  $75 \text{ Wh kg}^{-1}$ ,
- volumetric energy density approx.  $88 \text{ Wh L}^{-1}$ ,
- electrolyte volume approx.  $11 \text{ L kWh}^{-1}$ .

Compared to the LIB technology, the values for the ZMB technology (based on the amount of electrolyte) are significantly below the LIB values at the active materials level in the range of approx.  $300\text{--}400 \text{ Wh kg}^{-1}$  or approx.  $600\text{--}700 \text{ Wh L}^{-1}$  [93–95].

The energy density values of LIB at the module level are approx.  $200 \text{ Wh kg}^{-1}$  and  $350 \text{ Wh L}^{-1}$  [95,96]. Regarding the cell-to-module (gravimetric) efficiencies for LIB, the literature shows values of around 60–80% [97,98]. Comparing this to the active material-to-module level (active material-to-module), an efficiency of approx. 50% is shown [97,98]. This multiplier is only a rough estimate to extrapolate from the active material to the module level (taking into account, e.g., the housing, the wiring technology and the contacting). Nevertheless, this factor can also be used to estimate a potentially achievable energy density at module level for the ZMB technology, based on the calculated values at the active material level (see above), where the electrolyte is regarded as the active material of the ZMB. Taking into account the material-to-module efficiency of 50%, values of approx.  $38 \text{ Wh kg}^{-1}$  (and approx.  $44 \text{ Wh L}^{-1}$ ) can be calculated (based on the theoretical energy densities calculated above), being in the range of the lead-acid battery [96].

However, it must be pointed out that the use of a water-based electrolyte for the ZMB intrinsically leads to a lower energy density level due to the lower nominal cell voltage, but it does offer advantages regarding cost and safety. Additionally, there are further criteria coming up in particular for stationary applications (e.g., safety, specific costs, raw material availability, robustness, environmental compatibility), leading to power and energy density (especially in volumetric terms) playing a subordinate role in the stationary sector. Another topic is the possibilities for the aqueous ZMB technology in terms of the cell-to-module design and, one step further, on the pack level: Due to its high safety regarding the non-flammability of the aqueous electrolyte, peripheral safety devices such as protection circuit boards (PCB), positive thermal coefficient (PTC) elements, current-interrupt devices (CID) and fire-suppressing devices are not necessary [64]. Furthermore, a bipolar current collector design can be implemented [99,100]. Altogether, AZB have fewer inactive components at pack level, leading to advantages in terms of the energy density on the module and pack level compared to the LIB technology.

### 3.6. Power Density

ZMB use aqueous electrolytes with high ionic conductivities in the range of approx.  $50\text{--}60 \text{ mS cm}^{-2}$  for sulphate-based electrolytes (Supplementary Materials Table S4), which is an order of magnitude higher than LIB electrolytes [94]. This characteristic can act as a key enabler for high C-rates and good power densities of ZMB.

Nevertheless, the demand for C-rate capability depends on the application. For stationary use of ZMB systems (storage capacity < 10 kWh, e.g., home storage, off-grid storage), C-rates < 1 C are sufficient [101–104]. The same applies for frequency containment reserve systems in the MWh-scale. For peak shaving applications, the storage capacities are higher than home storage systems (approx. > 100 kWh), so even for high power outputs the C-rates can be less than 0.5 C [101–104].

On the other hand, the literature shows for ZMB that both battery and capacitor (C-rates > 10 C) applications are possible [83,105,106], showing the wide range of C-rate capability of the ZMB technology. Regarding the fields of application of ZMB, which should mainly be home/off-grid storage, frequency containment reserve and peak shaving, the power density should not be the key factor for the battery technology. Other factors such as low cost, high safety, raw material availability and environmental friendliness will be more in focus regarding the battery development.

### 3.7. Material Abundance and Sustainability

In view of the geopolitical situation, resource availability is once again coming more to the fore as an important criterion. The diversification of energy sources and carriers, as well as energy suppliers, makes energy supply more resilient to policy changes. The worldwide occurrence of zinc is 300 times greater than lithium [107,108], it can also be mined in Europe, and manganese is considered the most abundant element of all 3d transition metals in the Earth's crust [109], which makes them suitable candidates.

The electrolyte compositions for ZMB mainly use zinc salts such as  $ZnSO_4$ ,  $Zn(CH_3COO)_2$ ,  $Zn(CF_3SO_3)_2$ ,  $ZnCl_2$  or  $ZnBr_2$  (together with their corresponding manganese salts) [110]. Regarding the GHS for chemicals, most of those zinc salts are listed as harmful for humans (if swallowed) and toxic to aquatic life [111]. This collides with the claim of many publications in the field that ZMB is a non-toxic cell chemistry. Still, in comparison with other cell chemistries such as the LIB technology using organic electrolytes, the electrolyte components (e.g., DMC, EC, LiPF<sub>6</sub>, VC, etc.) are either flammable or can cause organ damage, which exceeds the GHS classifications for the ZMB components. As a result of this comparison, the term “toxicity” in the field of battery cell chemistries needs to be defined, especially regarding possible risk scenarios such as damage to the battery casing, flammability and thermal runaway, exposure to danger for humans, etc. Nevertheless, regarding the aforementioned points, the ZMB definitely shows advantages compared to the organic LIB technology.

In addition, battery recyclability is also coming to the fore, and for the ZMB it is possible to fall back on processes from the alkali-manganese battery that are already well established. Furthermore, the cell and module architecture can be designed to be modular and bipolar, which, together with the non-critical battery components, facilitates the recycling of the battery at the end-of-life stage [99,100]. Moreover, due to the non-flammable electrolyte, the danger of ignition during shredding in the recycling process is minimized.

## 4. Towards Practical Application of Zinc Manganese Batteries

Besides all the advantages and potential identified for ZMBs, this section focuses on the existing challenges towards practical application and discusses possible steps and approaches. Challenges exist at the cell level, which are shown schematically in Figure 8: Concerning the electrolyte development, the elementary tasks are the anode stability, also in connection with the hydrogen evolution, as well as the development of suitable host structures for manganese dioxide deposition that considers the low conductivity of the solid. In addition, we briefly present the extent to which model-based approaches can contribute here. Finally, we will discuss which special features are given regarding the extension on module level.

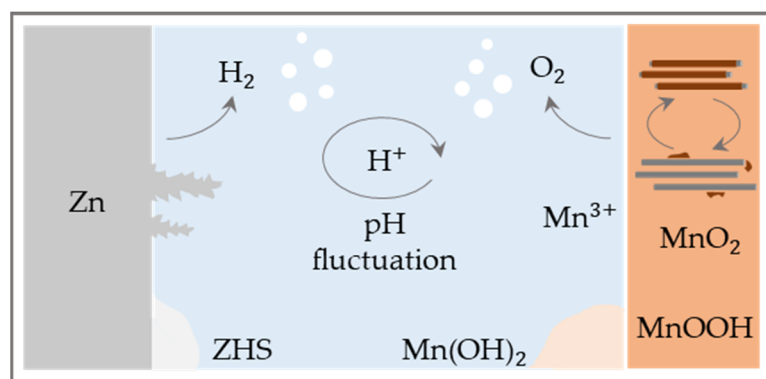


**Figure 8.** Challenges in the area of further development at cell level can be seen in anode stability, gas evolution, optimal support structures and stabilisation of the pH value.

#### 4.1. Cell-Level Engineering

The development of ZMB systems discussed in Section 2 illustrates the elementary influence of the electrolyte on the prevailing reaction mechanisms. The pH value in particular, but also the type of anion present and the concentration, which in turn have a strong influence on the solvation structure, play a decisive role. As has been pointed out, the accessibility of the two-electron mechanism at a mild pH has great potential. For this reason, electrolyte development with this background will be discussed in more detail below.

Studies have revealed the positive effect of using acetate anions compared to sulphate-based salts. Xie et al. show that the two-electron mechanism can be exploited by using manganese acetate and zinc acetate and attribute the change in reaction mechanism compared to  $\text{MnSO}_4$  to the coordination ability of acetate. The modified electrolyte is applied to a flow battery; however, a static battery is also investigated [61]. Similar observations are made by Zeng et al., where they attribute the positive effects to the strong adsorption effect of  $\text{CH}_3\text{COO}^-$  on the surface sites of  $\text{MnO}_2$  particles due to their high polarizability and electronegativity. Furthermore, compared to  $\text{CF}_3\text{SO}_3^-$  and  $\text{SO}_4^-$  anions, the acetate-based electrolyte showed improved properties regarding the Coulomb efficiency and cycling stability of the zinc electrodeposition [60].

Another positive effect achieved by the addition of acetate anions is given by the buffering effect with respect to pH changes, which is first highlighted by Mateos et al. and subsequently taken up by many research groups [59,86]. The anion can either be added directly via salt or via the addition as acid. In order to separate the effect of the addition of acid from the buffering property and the change in the concentration of free protons, Liu et al. investigated the effect of the addition of sulfuric acid in comparison with acetic acid and revealed that the latter significantly reduces the pH fluctuations and moreover effectively mitigates the corrosion and hydrogen evolution [55].

In addition to the use of electrolytes containing acetate, the stabilizing and positive effect could also be shown with other buffer substances [89]. The use of ammonium dihydrogen also leads to a suppression of pH fluctuations and the associated precipitation of ZHS and furthermore leads to the suppression of dendrite growth and side reactions [83]. Liu et al. also use phosphate-based buffers, although these are added directly via zinc hydrogen phosphate and not added as an electrolyte additive [112]. However, these also point to the special feature of the solid–liquid mechanism, which makes the electrolyte volume and the achievable concentration an essential property about the volumetric energy density. In addition, the solubility of the pH-stabilizing anions is also an important factor to provide sufficient effect even in realistic electrolyte volumes. One way to further increase the solubility is to introduce complexing agents and is followed by Huang et al., who use a 46.5 M  $\text{NH}_4\text{Ac}$  –  $\text{NH}_3$  –  $\text{Zn}(\text{Ac})_2$  –  $\text{Mn}(\text{Ac})$  electrolyte, with acetate to stabilize the desired reaction mechanisms, and  $\text{NH}_3$  and  $\text{NH}_4\text{Ac}$ , due to their strong complexation ability with

zinc and manganese ions, to prevent the solvation effect with the water molecules, thus improving the separation properties [92].

Furthermore, there is also the approach of decoupling the electrolyte ranges, so that the optimum pH value can be selected in each case regarding performance [113]. In this case, however, the different areas must be separated by suitable measures, such as jellification [57,113–115] or through special membranes [58,116,117], since otherwise they would mix due to diffusion processes. Shen et al., for example, use hydrogel electrolyte in which three layers with different pH values are applied on top of each other [115]. However, due to jellification, the overpotential is drastically increased, and ion crossover cannot be completely avoided, which leads to low voltage efficiency and poor cycling stability. In contrast, the use of the special ion-selective membranes is very expensive and the practical applicability must therefore be critically examined [114].

In addition to electrolyte development, the nature of the electrode structure also plays a significant role. Here, in particular, the achievable areal capacity is decisive for the attainable energy density, as this determines the ratio of active to passive material. Because manganese dioxide has only a moderate electric conductivity of  $10^{-4}$ – $10^{-3}$  S cm $^{-1}$  [118,119], the contact between the deposited layer and the current arrester strongly influences the performance. If the deposited layer becomes too thick, increased overvoltage is to be expected, which lowers the energy efficiency. This is solved by, e.g., using GLAD-ITO current collectors with a 3-dimensional structure, which shorten the diffusion routes and provide larger electroactive surface areas; therefore, compared to the 2D structure, significantly higher capacities can be achieved [86]. In addition, Mateos et al. emphasize the proper matching of the concentration of the reactants and the conversion rate, which are strongly linked to the cyclisation rate and the specific surface area.

For practical application, however, the considered loading of 0.028 mAh cm $^{-2}$  is clearly too low and overall represents the often only very low considered capacities in the literature below areal capacity of 0.616 mAh cm $^{-2}$  [120]. To further increase the surface area, many research groups use carbon felt/cloth [60,61,88,90] or other porous materials such as metal foams [120]. In addition, Lei et al. applied a mediator strategy with iodide to facilitate manganese dioxide dissolution and avoid exfoliated, “dead” MnO<sub>2</sub>, demonstrating an areal capacity of 50 mAh cm $^{-2}$  for a Zn–Mn redox flow battery [90]. Besides the absolute surface area, the texture and properties such as the hydrophilicity of the surface also play an important role [121]. Xie et al., for example, used a modified graphite fleece in which a slurry-coated carbon black layer is applied and achieved a smooth and uniform MnO<sub>2</sub> layer [61]. In addition, the electrodes are pre-treated with different methods, such as washing, and treated with different solutions or electrochemical methodologies [88,91].

In summary, it can be stated that promising approaches have been found to make the two-electrode mechanism accessible in the anode-friendly mild pH range, thus significantly minimizing the problems of corrosion and gas evolution of the anode in the acidic pH range and achieving promising cycle life and energy densities. In order to being made usable for practical applications, the experimental practices regarding cell construction must be more realistic in terms of electrolyte quantity, specific areal capacities and salt concentrations. In the further development, model-based approaches could also be useful to gain a better understanding of these complex processes and electrolyte compositions and their mass transport limitations in connection with the electrode structures, which will be discussed in more detail in the next section.

#### 4.2. Model-Based Development

In the field of LIBs, the model-based approach for cell development has long been established and makes an important contribution to the deeper understanding. However, since ZMBs are based on fundamentally different reaction mechanisms, traditional continuum models for LIB must be further developed to describe the specific processes in the cell. Here, the electrolyte not only serves to transport the ions, but also participates in the reaction as an active material. In contrast to intercalation, for underlying deposition

mechanism, a change in porosity with the charge state must also be taken into account. The behaviour of the ions in the neutral electrolyte is very complex and, as mentioned above, the mass transport limitations and the associated pH gradients within the cell have a fundamental influence on overpotential as well as the reaction mechanisms that take place. This makes it necessary to consider homogeneous reactions and the formation of complexes within the electrolyte.

To the best of our knowledge, there are currently almost no studies dealing with the performance in a neutral environment of ZMBs on the basis of modelling approaches and there is no implementation in which the important electrolyte relationships described above are represented [122]. However, experience in the field of zinc–air and flow batteries [123], geochemical processes [124] and water splitting [125] can be drawn upon. Clark et al., for example, use a continuum model to evaluate the performance of zinc–air batteries and optimize them in terms of pH stability, precipitation and energy density [126]. They point out the limitation of the buffer capacity due to mass transport and show that the electrolyte composition and concentration have a strong influence on the preferred precipitating salt. The solution of the system of equations is not trivial, since the concentrations of the species extend over several dimensions and even small additions of acids or bases have a strong influence on the prevailing complexes. Here, the time constants of the homogeneous reactions are significantly lower compared to transport and can thus be considered in thermodynamic equilibrium in a good approximation. The authors refer to this as the quasiparticle approach, although the “method of families” [123] or sequential non-iterative approach [124] is also used as a term [127]. For further development, the understanding and proper selection of different electrolyte compositions and their ability to control stable electrode–electrolyte transition is an important factor for which model-based development can potentially make an important contribution.

Another widely used model-based approach for the LIB technology is the representation based on equivalent circuit models (ECM). Compared to physical-based models, they are easier to implement and require less computing power. However, the identification of the necessary parameters can be very time-consuming, and the physical interpretability is not always given. Still, for LIBs with their well-investigated  $\text{Li}^+$  intercalation mechanism, the impedance spectra are usually modelled with a single equivalent circuit model (ECM) for different SOC [128–131]. In contrast, ZMBs show a different behaviour in terms of the reaction mechanisms with deposition/dissolution and intercalation mechanisms, gassing reactions and precipitation phenomena (Section 2). Therefore, another approach for ECM development can be suggested: For different SOC, different ECMS need to be created, as Bischoff, for example, shows in his investigations [132]. This approach is based on the suggestions regarding the different states in the ZMB during charging/discharging (Section 2) and can be summarized as follows (Figure 9):

- charged state (SOC ~100%): cathode coating (double-layer capacitance, constant-phase element, CPE) together with a  $\text{MnO}_2$  deposition on the cathode surface (diffusion resistance),
- intermediate state (SOC~80%): cathode coating (CPE) and dissolving  $\text{MnO}_2$  surface deposition (change in diffusion regime) and a precipitation of ZHS (growing double layer, CPE),
- discharged state (SOC~30/0%): cathode coating (CPE), dissolved  $\text{MnO}_2$  surface deposition (diffusion resistance disappeared) and a ZHS precipitation layer (new double layer, CPE),
- (ohmic) electrolyte resistance for all SOC.

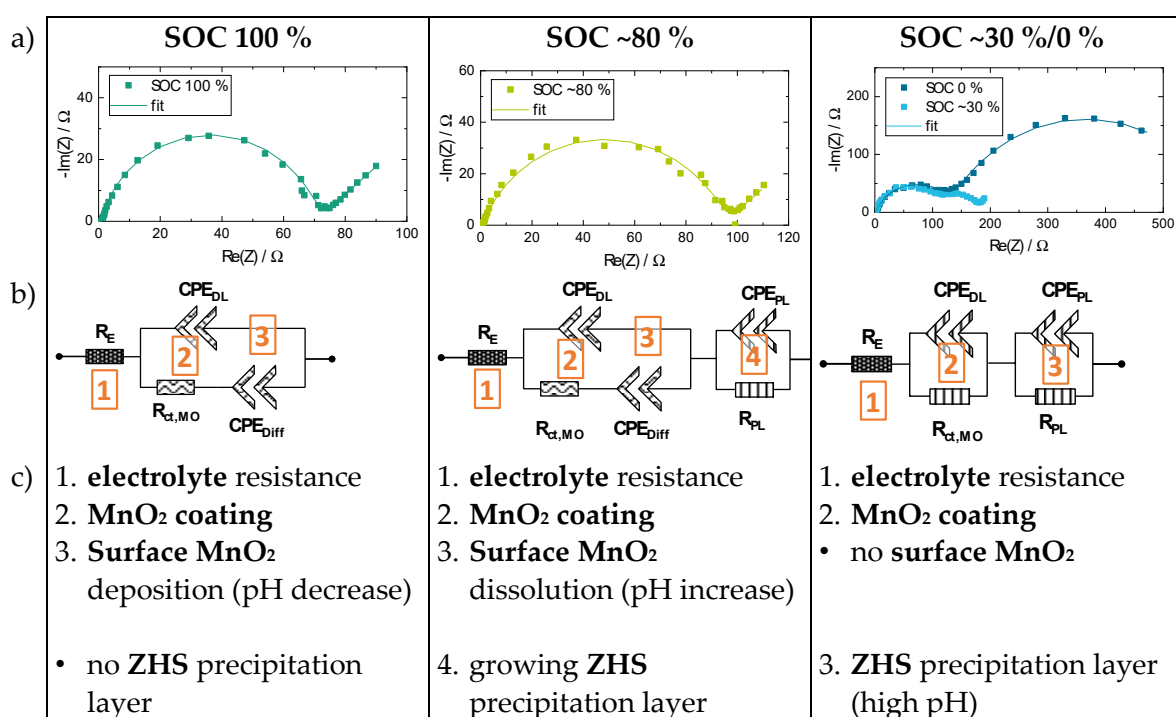


**Figure 9.** EIS spectra for a ZMB with 2 M ZnSO<sub>4</sub> + 0.1 M MnSO<sub>4</sub> electrolyte for different SOC 100/~/80/~/30/0%. (a). In relation to the change of the EIS spectra characteristics, the ECM are modified (b) and the corresponding elements are described (c). (excerpted and modified based on [132].)

The results of Bischoff show an increasing inner resistance of the ZMB cell from the charged to the discharged state of approx. one order of magnitude, which is confirmed with other ECM investigations in the literature [14,21,27,36]. Of course, this ECM approach only represents one possible interpretation of the EIS behaviour of the ZMB for different SOC. Furthermore, the EIS interpretation is highly dependent on the underlying reaction mechanism. Nevertheless, the interpretation approach described above points out the multiple reaction mechanisms in the aqueous ZMB with a significant contribution of the Mn<sup>2+</sup>/MnO<sub>2</sub> deposition/dissolution mechanism.

#### 4.3. Battery Module Development

In recent years, different approaches for developing zinc-based battery systems were published (Supplementary Materials Table S5). Still, to the best of our knowledge, there is no ZMB-based system available on the broad market yet.

At the early stage of the ZMB battery module research and regarding the challenges for the cyclability of the ZMB shown in this paper, a list of the major battery module components (e.g., battery module casing, electric components, electrodes, separator, electrolyte) and the respective demands and properties can be created (Figure 10). Within this list, the major challenges in terms of the electrochemical performance, such as the avoidance of side reactions at the anode side and the demands for the electrolyte in terms of the pH behaviour, are listed, amongst others. The list can be seen as a basis for the further application-oriented research and battery module development.

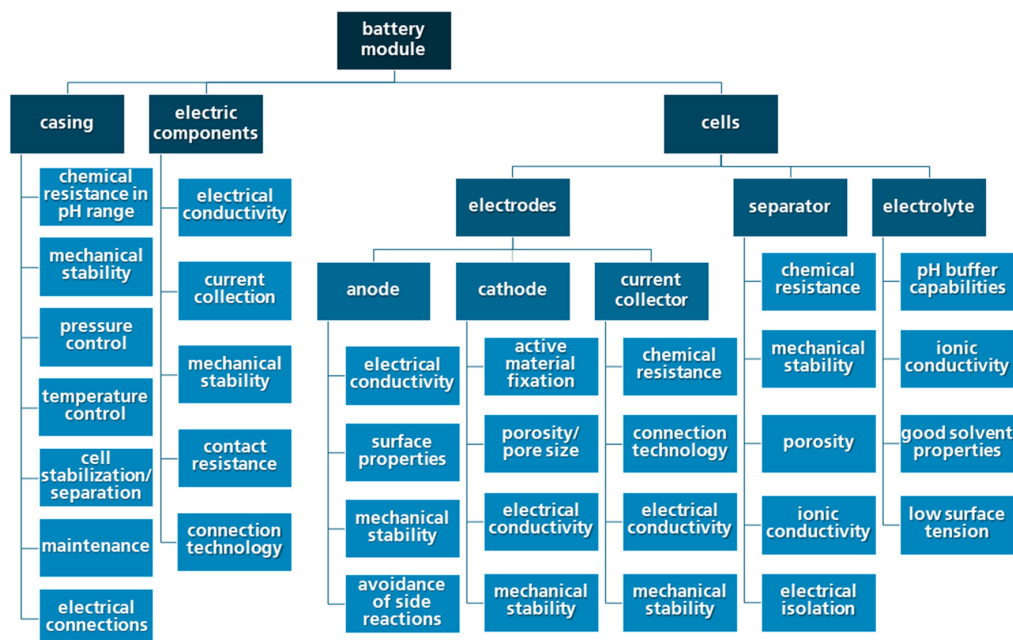


**Figure 10.** Overview of the main components of a ZMB module and the suggested properties and demands.

## 5. Conclusions

The energy transition and the need for intermediate storage with its various applications require re-evaluation of the different categories in the so called “Battery Ecosystem”. We present a battery system based on the material combination of zinc and manganese dioxide in mild aqueous electrolyte, being capable to cope with the high cost pressure for stationary applications. This battery technology also addresses the demands of abundant, cheap, and non-critical materials. In this regard, the presented battery technology deserves the attribute “green” in contrast to the dominant LIB technology. The new electrolyte approach with pH-stabilising properties is a crucial element for rechargeability. However, standardization in regard of experimental practice must be defined in order to improve comparability between promising approaches. In addition, the hydrogen evolution must be suppressed, which will be investigated in future research. Although the energy density of ZMB is much less than for LIB, the novel rechargeable ZMB could reach the magic USD 10 per kWh<sup>-1</sup> pack level limit, which is urgently required if batteries will become an important component in stationary applications and the energy transition. Altogether, this work classifies the current state of research in ZMB and emphasizes the potential of the ZMB technology, being capable of playing an outstanding role in the “Battery Ecosystem” for stationary energy storage in the future.

**Supplementary Materials:** The following supporting information can be downloaded at: <https://www.mdpi.com/article/10.3390/batteries9070367/s1>; Table S1: Reaction mechanisms in literature; Calculations S2: Energy density estimates; Table S3: C-rate calculations & transformations; Table S4: Ionic conductivity for ZMB electrolytes; Table S5: Industrial approaches for ZIB.

**Author Contributions:** Conceptualization, J.P.-B., O.F. and K.P.B.; methodology, J.P.-B., O.F. and K.P.B.; investigation, J.P.-B. and O.F.; writing—original draft preparation, J.P.-B., O.F., C.B. and K.P.B.; writing—review and editing, J.P.-B., O.F., C.B. and K.P.B.; visualization, J.P.-B., O.F. and C.B.; supervision, K.P.B. and D.B.; project administration, J.P.-B. and O.F.; funding acquisition, K.P.B. and D.B. All authors have read and agreed to the published version of the manuscript.

**Funding:** This research was funded by German Federal Ministry for Economics and Climate Action grant number [03EI3040D] and German Federal of Education and Research grant number [03SF0702B].

**Data Availability Statement:** No new data were created or analyzed in this study. Data sharing is not applicable to this article.

**Conflicts of Interest:** The authors declare no conflict of interest.

## References

1. Birke, P. (Ed.) *Modern Battery Engineering: A Comprehensive Introduction*; World Scientific Publishing: Hackensack, NJ, USA, 2019; ISBN 9789813272170.
2. Pavlov, D.D. *Lead-Acid Batteries: Science and Technology: A Handbook of Lead-Acid Battery Technology and Its Influence on the Product*, 2nd ed.; Elsevier: Amsterdam, The Netherlands, 2017; ISBN 9780444595522.
3. Soulopoulos, N.; Boers, M.; Fisher, R.; O'Donovan, A.; McKerracher, C. *Hitting the EV Inflection Point: Electric Vehicle Price Parity and Phasing out Combustion Vehicle Sales in Europe*; Bloomberg Finance L.P.: New York, NY, USA, 2021; Available online: [https://www.transportenvironment.org/wp-content/uploads/2021/08/2021\\_05\\_05\\_Electric\\_vehicle\\_price\\_parity\\_and\\_adoption\\_in\\_Europe\\_Final.pdf](https://www.transportenvironment.org/wp-content/uploads/2021/08/2021_05_05_Electric_vehicle_price_parity_and_adoption_in_Europe_Final.pdf) (accessed on 5 April 2023).
4. Kost, C.; Shammugam, S.; Fluri, V.; Peper, D.; Memar, A.D.; Schlegl, T. *Levelized Cost of Electricity Renewable Energy Technologies*; Fraunhofer Institute for Solar Energy Systems ISE: Freiburg, Germany; Available online: [https://www.ise.fraunhofer.de/content/dam/ise/en/documents/publications/studies/EN2021\\_Fraunhofer-ISE\\_LCOE\\_Renewable\\_Energy\\_Technologies.pdf](https://www.ise.fraunhofer.de/content/dam/ise/en/documents/publications/studies/EN2021_Fraunhofer-ISE_LCOE_Renewable_Energy_Technologies.pdf) (accessed on 21 April 2023).
5. Hornsdale Power Reserve—South Australia's Big Battery. Available online: <https://hornsdalepowerreserve.com.au/> (accessed on 20 April 2023).
6. Leclanché, G. Quelques Observations sur L'emploi des Piles Électriques. *Les Mondes* [Online], 1868. Available online: <https://gallica.bnf.fr/ark:/12148/bpt6k62094v/f2.image> (accessed on 5 April 2023).
7. Gassner, C., Jr. Galvanic Battery 383064. U.S. Patent US373064A, 20 May 1887.
8. Marsala, P.A.; Kordesch, K.; Lewis, U.F. Dry Cell. U.S. Patent US2960558A, 10 September 1957.
9. Kordesch, K.; Gsellmann, J.; Peri, M.; Tomantschger, K.; Chemelli, R. The rechargeability of manganese dioxide in alkaline electrolyte. *Electrochim. Acta* **1981**, *26*, 1495–1504. [[CrossRef](#)]
10. Yamamoto, T.; Shoji, T. Rechargeable Zn|ZnSO<sub>4</sub>|MnO<sub>2</sub>-type cells. *Inorg. Chim. Acta* **1986**, *117*, L27–L28. [[CrossRef](#)]
11. Reddy, M.V.; Mauger, A.; Julien, C.M.; Paolella, A.; Zaghib, K. Brief History of Early Lithium-Battery Development. *Materials* **2020**, *13*, 1884. [[CrossRef](#)] [[PubMed](#)]
12. Xu, C.; Li, B.; Du, H.; Kang, F. Energetic zinc ion chemistry: The rechargeable zinc ion battery. *Angew. Chem.* **2012**, *51*, 933–935. [[CrossRef](#)] [[PubMed](#)]
13. Xu, C.; Du, H.; Li, B.; Kang, F.; Zeng, Y. Reversible Insertion Properties of Zinc Ion into Manganese Dioxide and Its Application for Energy Storage. *Electrochim. Solid State Lett.* **2009**, *12*, A61. [[CrossRef](#)]
14. Xu, C.; Chiang, S.W.; Ma, J.; Kang, F. Investigation on Zinc Ion Storage in Alpha Manganese Dioxide for Zinc Ion Battery by Electrochemical Impedance Spectrum. *J. Electrochem. Soc.* **2012**, *160*, A93–A97. [[CrossRef](#)]
15. Xu, D.; Li, B.; Wei, C.; He, Y.-B.; Du, H.; Chu, X.; Qin, X.; Yang, Q.-H.; Kang, F. Preparation and Characterization of MnO<sub>2</sub>/acid-treated CNT Nanocomposites for Energy Storage with Zinc Ions. *Electrochim. Acta* **2014**, *133*, 254–261. [[CrossRef](#)]
16. Alfaruqi, M.H.; Gim, J.; Kim, S.; Song, J.; Pham, D.T.; Jo, J.; Xiu, Z.; Mathew, V.; Kim, J. A layered δ-MnO<sub>2</sub> nanoflake cathode with high zinc-storage capacities for eco-friendly battery applications. *Electrochim. Commun.* **2015**, *60*, 121–125. [[CrossRef](#)]
17. Alfaruqi, M.H.; Mathew, V.; Gim, J.; Kim, S.; Song, J.; Baboo, J.P.; Choi, S.H.; Kim, J. Electrochemically Induced Structural Transformation in a γ-MnO<sub>2</sub> Cathode of a High Capacity Zinc-Ion Battery System. *Chem. Mater.* **2015**, *27*, 3609–3620. [[CrossRef](#)]
18. Alfaruqi, M.H.; Gim, J.; Kim, S.; Song, J.; Jo, J.; Kim, S.; Mathew, V.; Kim, J. Enhanced reversible divalent zinc storage in a structurally stable α-MnO<sub>2</sub> nanorod electrode. *J. Power Sources* **2015**, *288*, 320–327. [[CrossRef](#)]
19. Alfaruqi, M.H.; Islam, S.; Gim, J.; Song, J.; Kim, S.; Pham, D.T.; Jo, J.; Xiu, Z.; Mathew, V.; Kim, J. A high surface area tunnel-type α-MnO<sub>2</sub> nanorod cathode by a simple solvent-free synthesis for rechargeable aqueous zinc-ion batteries. *Chem. Phys. Lett.* **2016**, *650*, 64–68. [[CrossRef](#)]
20. Zhang, N.; Cheng, F.; Liu, Y.; Zhao, Q.; Lei, K.; Chen, C.; Liu, X.; Chen, J. Cation-Deficient Spinel ZnMn<sub>2</sub>O<sub>4</sub> Cathode in Zn(CF<sub>3</sub>SO<sub>3</sub>)<sub>2</sub> Electrolyte for Rechargeable Aqueous Zn-Ion Battery. *J. Am. Chem. Soc.* **2016**, *138*, 12894–12901. [[CrossRef](#)] [[PubMed](#)]
21. Sun, W.; Wang, F.; Hou, S.; Yang, C.; Fan, X.; Ma, Z.; Gao, T.; Han, F.; Hu, R.; Zhu, M.; et al. Zn/MnO<sub>2</sub> Battery Chemistry With H<sup>+</sup> and Zn<sup>2+</sup> Coininsertion. *J. Am. Chem. Soc.* **2017**, *139*, 9775–9778. [[CrossRef](#)] [[PubMed](#)]
22. Zhang, N.; Cheng, F.; Liu, J.; Wang, L.; Long, X.; Liu, X.; Li, F.; Chen, J. Rechargeable aqueous zinc-manganese dioxide batteries with high energy and power densities. *Nat. Commun.* **2017**, *8*, 405. [[CrossRef](#)]
23. Chamoun, M.; Brant, W.R.; Tai, C.-W.; Karlsson, G.; Noréus, D. Rechargeability of aqueous sulfate Zn/MnO<sub>2</sub> batteries enhanced by accessible Mn<sup>2+</sup> ions. *Energy Storage Mater.* **2018**, *15*, 351–360. [[CrossRef](#)]
24. Alfaruqi, M.H.; Islam, S.; Putro, D.Y.; Mathew, V.; Kim, S.; Jo, J.; Kim, S.; Sun, Y.-K.; Kim, K.; Kim, J. Structural transformation and electrochemical study of layered MnO<sub>2</sub> in rechargeable aqueous zinc-ion battery. *Electrochim. Acta* **2018**, *276*, 1–11. [[CrossRef](#)]
25. Hao, J.; Mou, J.; Zhang, J.; Dong, L.; Liu, W.; Xu, C.; Kang, F. Electrochemically induced spinel-layered phase transition of Mn<sub>3</sub>O<sub>4</sub> in high performance neutral aqueous rechargeable zinc battery. *Electrochim. Acta* **2018**, *259*, 170–178. [[CrossRef](#)]

26. Wu, B.; Zhang, G.; Yan, M.; Xiong, T.; He, P.; He, L.; Xu, X.; Mai, L. Graphene Scroll-Coated  $\alpha$ -MnO<sub>2</sub> Nanowires as High-Performance Cathode Materials for Aqueous Zn-Ion Battery. *Small* **2018**, *14*, e1703850. [CrossRef]
27. Li, Y.; Wang, S.; Salvador, J.R.; Wu, J.; Liu, B.; Yang, W.; Yang, J.; Zhang, W.; Liu, J.; Yang, J. Reaction Mechanisms for Long-Life Rechargeable Zn/MnO<sub>2</sub> Batteries. *Chem. Mater.* **2019**, *31*, 2036–2047. [CrossRef]
28. Wang, X.; Zheng, S.; Zhou, F.; Qin, J.; Shi, X.; Wang, S.; Sun, C.; Bao, X.; Wu, Z.-S. Scalable fabrication of printed Zn//MnO<sub>2</sub> planar micro-batteries with high volumetric energy density and exceptional safety. *Natl. Sci. Rev.* **2020**, *7*, 64–72. [CrossRef]
29. Yang, S.; Zhang, M.; Wu, X.; Wu, X.; Zeng, F.; Li, Y.; Duan, S.; Fan, D.; Yang, Y.; Wu, X. The excellent electrochemical performances of ZnMn<sub>2</sub>O<sub>4</sub>/Mn<sub>2</sub>O<sub>3</sub>: The composite cathode material for potential aqueous zinc ion batteries. *J. Electroanal. Chem.* **2019**, *832*, 69–74. [CrossRef]
30. Qiu, C.; Zhu, X.; Xue, L.; Ni, M.; Zhao, Y.; Liu, B.; Xia, H. The function of Mn<sup>2+</sup> additive in aqueous electrolyte for Zn//MnO<sub>2</sub> battery. *Electrochim. Acta* **2020**, *351*, 136445. [CrossRef]
31. Khamsanga, S.; Pornprasertsuk, R.; Yonezawa, T.; Mohamad, A.A.; Kheawhom, S.  $\delta$ -MnO<sub>2</sub> nanoflower/graphite cathode for rechargeable aqueous zinc ion batteries. *Sci. Rep.* **2019**, *9*, 8441. [CrossRef] [PubMed]
32. Ko, J.S.; Sassin, M.B.; Parker, J.F.; Rolison, D.R.; Long, J.W. Combining battery-like and pseudocapacitive charge storage in 3D MnO x @carbon electrode architectures for zinc-ion cells. *Sustainable Energy Fuels* **2018**, *2*, 626–636. [CrossRef]
33. Lee, J.; Ju, J.B.; Cho, W.I.; Cho, B.W.; Oh, S.H. Todorokite-type MnO<sub>2</sub> as a zinc-ion intercalating material. *Electrochim. Acta* **2013**, *112*, 138–143. [CrossRef]
34. Lee, B.; Yoon, C.S.; Lee, H.R.; Chung, K.Y.; Cho, B.W.; Oh, S.H. Electrochemically-induced reversible transition from the tunneled to layered polymorphs of manganese dioxide. *Sci. Rep.* **2014**, *4*, 6066. [CrossRef]
35. Lee, B.; Seo, H.R.; Lee, H.R.; Yoon, C.S.; Kim, J.H.; Chung, K.Y.; Cho, B.W.; Oh, S.H. Critical Role of pH Evolution of Electrolyte in the Reaction Mechanism for Rechargeable Zinc Batteries. *ChemSusChem* **2016**, *9*, 2948–2956. [CrossRef]
36. Guo, X.; Zhou, J.; Bai, C.; Li, X.; Fang, G.; Liang, S. Zn/MnO<sub>2</sub> battery chemistry with dissolution-deposition mechanism. *Mater. Today Energy* **2020**, *16*, 100396. [CrossRef]
37. Li, L.; Hoang, T.K.A.; Zhi, J.; Han, M.; Li, S.; Chen, P. Functioning Mechanism of the Secondary Aqueous Zn- $\beta$ -MnO<sub>2</sub> Battery. *ACS Appl. Mater. Interfaces* **2020**, *12*, 12834–12846. [CrossRef]
38. Huang, Y.; Mou, J.; Liu, W.; Wang, X.; Dong, L.; Kang, F.; Xu, C. Novel Insights into Energy Storage Mechanism of Aqueous Rechargeable Zn/MnO<sub>2</sub> Batteries with Participation of Mn<sup>2+</sup>. *Nano Micro Lett.* **2019**, *11*, 860. [CrossRef]
39. Bischoff, C.F.; Fitz, O.S.; Burns, J.; Bauer, M.; Gentischer, H.; Birke, K.P.; Henning, H.-M.; Biro, D. Revealing the Local pH Value Changes of Acidic Aqueous Zinc Ion Batteries with a Manganese Dioxide Electrode during Cycling. *J. Electrochem. Soc.* **2020**, *167*, 20545. [CrossRef]
40. Pan, H.; Shao, Y.; Yan, P.; Cheng, Y.; Han, K.S.; Nie, Z.; Wang, C.; Yang, J.; Li, X.; Bhattacharya, P.; et al. Reversible aqueous zinc/manganese oxide energy storage from conversion reactions. *Nat. Energy* **2016**, *1*, 16039. [CrossRef]
41. Chao, D.; Zhou, W.; Ye, C.; Zhang, Q.; Chen, Y.; Gu, L.; Davey, K.; Qiao, S.-Z. An Electrolytic Zn-MnO<sub>2</sub> Battery for High-Voltage and Scalable Energy Storage. *Angew. Chem. Int. Ed.* **2019**, *58*, 7823–7828. [CrossRef] [PubMed]
42. Li, G.; Chen, W.; Zhang, H.; Gong, Y.; Shi, F.; Wang, J.; Zhang, R.; Chen, G.; Jin, Y.; Wu, T.; et al. Membrane-Free Zn/MnO<sub>2</sub> Flow Battery for Large-Scale Energy Storage. *Adv. Energy Mater.* **2020**, *10*, 1902085. [CrossRef]
43. Fitz, O.; Bischoff, C.; Bauer, M.; Gentischer, H.; Birke, K.P.; Henning, H.-M.; Biro, D. Electrolyte Study with in Operando pH Tracking Providing Insight into the Reaction Mechanism of Aqueous Acidic Zn//MnO<sub>2</sub> Batteries. *ChemElectroChem* **2021**, *8*, 3553–3566. [CrossRef]
44. Weast, R.C. *CRC Handbook of Chemistry and Physics: A Ready-Reference Book of Chemical and Physical Data*, 97th ed.; Haynes, W.M., Ed.; CRC Press: Boca Raton, FL, USA, 2017; ISBN 9781498754286.
45. Kim, Y.-S.; Harris, K.D.; Limoges, B.; Balland, V. On the unsuspected role of multivalent metal ions on the charge storage of a metal oxide electrode in mild aqueous electrolytes. *Chem. Sci.* **2019**, *10*, 8752–8763. [CrossRef] [PubMed]
46. Balland, V.; Mateos, M.; Singh, A.; Harris, K.D.; Laberty-Robert, C.; Limoges, B. The Role of Al<sup>3+</sup>-Based Aqueous Electrolytes in the Charge Storage Mechanism of MnOx Cathodes. *Small* **2021**, *17*, e2101515. [CrossRef]
47. Chen, H.; Cai, S.; Wu, Y.; Wang, W.; Xu, M.; Bao, S.-J. Successive electrochemical conversion reaction to understand the performance of aqueous Zn/MnO<sub>2</sub> batteries with Mn<sup>2+</sup> additive. *Mater. Today Energy* **2021**, *20*, 100646. [CrossRef]
48. Shen, X.; Wang, X.; Zhou, Y.; Shi, Y.; Zhao, L.; Jin, H.; Di, J.; Li, Q. Highly Reversible Aqueous Zn-MnO<sub>2</sub> Battery by Supplementing Mn<sup>2+</sup>-Mediated MnO<sub>2</sub> Deposition and Dissolution. *Adv. Funct. Mater.* **2021**, *31*, 2101579. [CrossRef]
49. Perez-Antolin, D.; Sáez-Bernal, I.; Colina, A.; Ventosa, E. Float-charging protocol in rechargeable Zn-MnO<sub>2</sub> batteries: Unraveling the key role of Mn<sup>2+</sup> additives in preventing spontaneous pH changes. *Electrochim. Commun.* **2022**, *138*, 107271. [CrossRef]
50. Liang, G.; Mo, F.; Li, H.; Tang, Z.; Liu, Z.; Wang, D.; Yang, Q.; Ma, L.; Zhi, C. A Universal Principle to Design Reversible Aqueous Batteries Based on Deposition-Dissolution Mechanism. *Adv. Energy Mater.* **2019**, *9*, 1901838. [CrossRef]
51. Pourbaix, M. *Atlas of Electrochemical Equilibria in Aqueous Solutions*, 2nd ed.; NACE International: Houston, TX, USA, 1974; ISBN 0915567989.
52. Kim, S.H.; Oh, S.M. Degradation mechanism of layered MnO<sub>2</sub> cathodes in Zn/ZnSO<sub>4</sub>/MnO<sub>2</sub> rechargeable cells. *J. Power Sources* **1998**, *72*, 150–158. [CrossRef]
53. Atkins, P.W.; de Paula, J. *Physical Chemistry*, 9th ed.; W.H. Freeman and Company: New York, NY, USA, 2010; ISBN 9781429218122.

54. Mainar, A.R.; Iruin, E.; Colmenares, L.C.; Kvasha, A.; de Meatza, I.; Bengoechea, M.; Leonet, O.; Boyano, I.; Zhang, Z.; Blazquez, J.A. An overview of progress in electrolytes for secondary zinc-air batteries and other storage systems based on zinc. *J. Energy Storage* **2018**, *15*, 304–328. [CrossRef]
55. Wang, N.; Qiu, X.; Xu, J.; Huang, J.; Cao, Y.; Wang, Y. Cathode Materials Challenge Varied with Different Electrolytes in Zinc Batteries. *ACS Mater. Lett.* **2022**, *4*, 190–204. [CrossRef]
56. Shin, J.; Lee, J.; Park, Y.; Choi, J.W. Aqueous zinc ion batteries: Focus on zinc metal anodes. *Chem. Sci.* **2020**, *11*, 2028–2044. [CrossRef] [PubMed]
57. Tang, H.; Yin, Y.; Huang, Y.; Wang, J.; Liu, L.; Qu, Z.; Zhang, H.; Li, Y.; Zhu, M.; Schmidt, O.G. Battery-Everywhere Design Based on a Cathodeless Configuration with High Sustainability and Energy Density. *ACS Energy Lett.* **2021**, *6*, 1859–1868. [CrossRef]
58. Liu, C.; Chi, X.; Han, Q.; Liu, Y. A High Energy Density Aqueous Battery Achieved by Dual Dissolution/Deposition Reactions Separated in Acid-Alkaline Electrolyte. *Adv. Energy Mater.* **2020**, *10*, 1903589. [CrossRef]
59. Mateos, M.; Makivic, N.; Kim, Y.-S.; Limoges, B.; Balland, V. Accessing the Two-Electron Charge Storage Capacity of MnO<sub>2</sub> in Mild Aqueous Electrolytes. *Adv. Energy Mater.* **2020**, *10*, 2000332. [CrossRef]
60. Zeng, X.; Liu, J.; Mao, J.; Hao, J.; Wang, Z.; Zhou, S.; Ling, C.D.; Guo, Z. Toward a Reversible Mn<sup>4+</sup>/Mn<sup>2+</sup> Redox Reaction and Dendrite-Free Zn Anode in Near-Neutral Aqueous Zn/MnO<sub>2</sub> Batteries via Salt Anion Chemistry. *Adv. Energy Mater.* **2020**, *10*, 1904163. [CrossRef]
61. Xie, C.; Li, T.; Deng, C.; Song, Y.; Zhang, H.; Li, X. A highly reversible neutral zinc/manganese battery for stationary energy storage. *Energy Environ. Sci.* **2020**, *13*, 135–143. [CrossRef]
62. Naser, J.; Mjalli, F.S.; Gano, Z.S. Molar heat capacity of tetrabutylammonium chloride-based deep eutectic solvents and their binary water mixtures. *Asia Pac. J. Chem. Eng.* **2017**, *12*, 938–947. [CrossRef]
63. Wittman, R.M.; Perry, M.L.; Lambert, T.N.; Chalamala, B.R.; Preger, Y. Perspective—On the Need for Reliability and Safety Studies of Grid-Scale Aqueous Batteries. *J. Electrochem. Soc.* **2020**, *167*, 90545. [CrossRef]
64. Song, J.; Xu, K.; Liu, N.; Reed, D.; Li, X. Crossroads in the renaissance of rechargeable aqueous zinc batteries. *Mater. Today* **2021**, *45*, 191–212. [CrossRef]
65. Emilsson, E.; Dahllöf, L. *Lithium-Ion Vehicle Battery Production: Status 2019 on Energy Use, CO<sub>2</sub> Emissions, Use of Metals, Products Environmental Footprint, and Recycling*; LVL Swedish Environmental Research Institute Ltd.: Stockholm, Sweden, 2019.
66. Lambert, T.N. Zn/MnO<sub>2</sub> Batteries; Sandia National Lab. (SNL-NM): Albuquerque, NM, USA, 2020. Available online: <https://www.osti.gov/servlets/purl/1822637> (accessed on 1 October 2020).
67. Li, Z.; Pan, M.S.; Su, L.; Tsai, P.-C.; Badel, A.F.; Valle, J.M.; Eiler, S.L.; Xiang, K.; Brushett, F.R.; Chiang, Y.-M. Air-Breathing Aqueous Sulfur Flow Battery for Ultralow-Cost Long-Duration Electrical Storage. *Joule* **2017**, *1*, 306–327. [CrossRef]
68. Spoerke, E.D.; Passell, H.; Cowles, G.; Lambert, T.N.; Yadav, G.G.; Huang, J.; Banerjee, S.; Chalamala, B. Driving Zn-MnO<sub>2</sub> grid-scale batteries: A roadmap to cost-effective energy storage. *MRS Energy Sustain.* **2022**, *9*, 13–18. [CrossRef]
69. Lim, M.B.; Lambert, T.N.; Chalamala, B.R. Rechargeable alkaline zinc–manganese oxide batteries for grid storage: Mechanisms, challenges and developments. *Mater. Sci. Eng. R Rep.* **2021**, *143*, 100593. [CrossRef]
70. Bellini, E. Salient Energy Develops Zinc-Ion Battery for Residential Applications, United States. Available online: <https://pv-magazine-usa.com/2022/04/21/salient-energy-develops-zinc-ion-battery-for-residential-applications/> (accessed on 20 April 2023).
71. Adams, B.D. Electrolyte Additives for Zinc Metal Electrodes. U.S. Patent 16/500,223, 1 May 2018. Available online: <https://patentimages.storage.googleapis.com/69/77/81/d206e430691f7b/US20200176198A1.pdf> (accessed on 20 April 2023).
72. Enerpoly, A.B. Enerpoly: Sustainable Batteries for Energy Storage. Available online: <https://enerpoly.com/> (accessed on 27 May 2022).
73. Eos Energy Enterprises. Available online: <https://eosenergystorage.com/> (accessed on 30 May 2022).
74. Adams, B.D.; Kundu, D.; Nazar, L.F. Electrode Materials for Rechargeable Zinc Cells and Batteries Produced Therefrom. U.S. Patent 9,780,412B2, 31 May 2016. Available online: <https://patentimages.storage.googleapis.com/02/f8/3b/846694b7dbba8a/WO2016197236A1.pdf> (accessed on 20 April 2023).
75. Kundu, D.; Adams, B.D.; Duffort, V.; Vajargah, S.H.; Nazar, L.F. A high-capacity and long-life aqueous rechargeable zinc battery using a metal oxide intercalation cathode. *Nat. Energy* **2016**, *1*, 16119. [CrossRef]
76. Spector, J. Zinc Battery Startup Eos Kept Afloat in a Lithium-Ion World. Is It Ready for the Public Markets? Boston, MA, USA, 2020. Available online: <https://www.greentechmedia.com/articles/read/can-zinc-battery-startup-eos-succeed-in-public-markets> (accessed on 20 April 2023).
77. Steingart, D.A.; Chamoun, M.; Hertzberg, B.; Davies, G.; Hsieh, A.G. Hyper-Dendritic Nanoporous Zinc Foam Anodes, Methods of Producing the Same, and Methods for Their Use. U.S. Patent 15/049,489, 22 February 2016. Available online: <https://patentimages.storage.googleapis.com/91/df/10/248b433788d210/US20170025677A1.pdf> (accessed on 20 April 2023).
78. McClanahan, A. Urban Electric Power Takes Energy Storage from Startup to Grid-Scale, Washington DC, USA, 2022. Available online: <https://arpa-e.energy.gov/news-and-media/blog-posts/urban-electric-power-takes-energy-storage-startup-grid-scale> (accessed on 20 April 2023).
79. Urban Electric Power. Available online: <https://urbanelectricpower.com/> (accessed on 27 May 2022).

80. Srivastava, S. Comprehensive Microgrid Energy Storage Designs with Guaranteed Optimality: ESTCP Project EW19-5054, Alexandria, VA, USA, 2020. Available online: <https://www.serdp-estcp.org/content/download/52270/514263/file/EW19-5054%20Final%20Report.pdf> (accessed on 27 May 2022).
81. Liu, Z.; Huang, Y.; Huang, Y.; Yang, Q.; Li, X.; Huang, Z.; Zhi, C. Voltage issue of aqueous rechargeable metal-ion batteries. *Chem. Soc. Rev.* **2019**, *49*, 180–232. [CrossRef]
82. Jia, X.; Liu, C.; Neale, Z.G.; Yang, J.; Cao, G. Active Materials for Aqueous Zinc Ion Batteries: Synthesis, Crystal Structure, Morphology, and Electrochemistry. *Chem. Rev.* **2020**, *120*, 7795–7866. [CrossRef]
83. Zhang, W.; Dai, Y.; Chen, R.; Xu, Z.; Li, J.; Zong, W.; Li, H.; Li, Z.; Zhang, Z.; Zhu, J.; et al. Highly Reversible Zinc Metal Anode in a Dilute Aqueous Electrolyte Enabled by a pH Buffer Additive. *Angew. Chem. Int. Ed.* **2023**, *62*, e202212695. [CrossRef]
84. Wang, L.; Zheng, J. Recent advances in cathode materials of rechargeable aqueous zinc-ion batteries. *Mater. Today Adv.* **2020**, *7*, 100078. [CrossRef]
85. Wang, D.; Wang, L.; Liang, G.; Li, H.; Liu, Z.; Tang, Z.; Liang, J.; Zhi, C. A Superior  $\delta$ -MnO<sub>2</sub> Cathode and a Self-Healing Zn- $\delta$ -MnO<sub>2</sub> Battery. *ACS Nano* **2019**, *13*, 10643–10652. [CrossRef] [PubMed]
86. Mateos, M.; Harris, K.D.; Limoges, B.; Balland, V. Nanostructured Electrode Enabling Fast and Fully Reversible MnO<sub>2</sub>-to-Mn<sup>2+</sup> Conversion in Mild Buffered Aqueous Electrolytes. *ACS Appl. Energy Mater.* **2020**, *3*, 7610–7618. [CrossRef]
87. Huang, S.; Zhu, J.; Tian, J.; Niu, Z. Recent Progress in the Electrolytes of Aqueous Zinc-Ion Batteries. *Chem. Eur. J.* **2019**, *25*, 14480–14494. [CrossRef]
88. Liu, Z.; Yang, Y.; Liang, S.; Lu, B.; Zhou, J. pH-Buffer Contained Electrolyte for Self-Adjusted Cathode-Free Zn-MnO<sub>2</sub> Batteries with Coexistence of Dual Mechanisms. *Small Struct.* **2021**, *2*, 2100119. [CrossRef]
89. Molaei, E.; Doroodmand, M.M.; Shaali, R. Tartaric acid as a novel additive for approaching high-performance capacity retention in zinc-ion battery. *Sci. Rep.* **2022**, *12*, 13301. [CrossRef]
90. Lei, J.; Yao, Y.; Wang, Z.; Lu, Y.-C. Towards high-areal-capacity aqueous zinc–manganese batteries: Promoting MnO<sub>2</sub> dissolution by redox mediators. *Energy Environ. Sci.* **2021**, *14*, 4418–4426. [CrossRef]
91. Liu, Y.; Qin, Z.; Yang, X.; Liu, J.; Liu, X.-X.; Sun, X. High-Voltage Manganese Oxide Cathode with Two-Electron Transfer Enabled by a Phosphate Proton Reservoir for Aqueous Zinc Batteries. *ACS Energy Lett.* **2022**, *7*, 1814–1819. [CrossRef]
92. Huang, J.; Chi, X.; Wu, J.; Liu, J.; Liu, Y. High-concentration dual-complex electrolyte enabled a neutral aqueous zinc-manganese electrolytic battery with superior stability. *Chem. Eng. J.* **2022**, *430*, 133058. [CrossRef]
93. Baumann, M.; Häring, M.; Schmidt, M.; Schneider, L.; Peters, J.F.; Bauer, W.; Binder, J.R.; Weil, M. Prospective Sustainability Screening of Sodium-Ion Battery Cathode Materials. *Adv. Energy Mater.* **2022**, *12*, 2202636. [CrossRef]
94. Armand, M.; Axmann, P.; Bresser, D.; Copley, M.; Edström, K.; Ekberg, C.; Guyomard, D.; Lestriez, B.; Novák, P.; Petranikova, M.; et al. Lithium-ion batteries—Current state of the art and anticipated developments. *J. Power Sources* **2020**, *479*, 228708. [CrossRef]
95. Fan, X.; Liu, B.; Liu, J.; Ding, J.; Han, X.; Deng, Y.; Lv, X.; Xie, Y.; Chen, B.; Hu, W.; et al. Battery Technologies for Grid-Level Large-Scale Electrical Energy Storage. *Trans. Tianjin Univ.* **2020**, *26*, 92–103. [CrossRef]
96. May, G.J.; Davidson, A.; Monahov, B. Lead batteries for utility energy storage: A review. *J. Energy Storage* **2018**, *15*, 145–157. [CrossRef]
97. Löbberding, H.; Wessel, S.; Offermanns, C.; Kehrer, M.; Rother, J.; Heimes, H.; Kampker, A. From Cell to Battery System in BEVs: Analysis of System Packing Efficiency and Cell Types. *World Electr. Veh. J.* **2020**, *11*, 77. [CrossRef]
98. Yang, X.-G.; Liu, T.; Wang, C.-Y. Thermally modulated lithium iron phosphate batteries for mass-market electric vehicles. *Nat. Energy* **2021**, *6*, 176–185. [CrossRef]
99. Evanko, B.; Yoo, S.J.; Lipton, J.; Chun, S.-E.; Moskovits, M.; Ji, X.; Boettcher, S.W.; Stucky, G.D. Stackable bipolar pouch cells with corrosion-resistant current collectors enable high-power aqueous electrochemical energy storage. *Energy Environ. Sci.* **2018**, *11*, 2865–2875. [CrossRef]
100. Xue, T.; Fan, H.J. From aqueous Zn-ion battery to Zn-MnO<sub>2</sub> flow battery: A brief story. *J. Energy Chem.* **2021**, *54*, 194–201. [CrossRef]
101. Kućević, D.; Tepe, B.; Englberger, S.; Parlikar, A.; Mühlbauer, M.; Bohlen, O.; Jossen, A.; Hesse, H. Standard battery energy storage system profiles: Analysis of various applications for stationary energy storage systems using a holistic simulation framework. *J. Energy Storage* **2020**, *28*, 101077. [CrossRef]
102. Figgener, J.; Stenzel, P.; Kairies, K.-P.; Linßen, J.; Haberschusz, D.; Wessels, O.; Robinius, M.; Stolten, D.; Sauer, D.U. The development of stationary battery storage systems in Germany—Status 2020. *J. Energy Storage* **2021**, *33*, 101982. [CrossRef]
103. European Commission. *Batteries Europe. Roadmap on Stationary Applications for Batteries: Prepared by Working Group 6*; European Commission: Brussels, Belgium, 2022; Available online: <https://energy.ec.europa.eu/system/files/2022-01/vol-6-009.pdf> (accessed on 14 April 2023).
104. Campana, P.E.; Cioccolanti, L.; François, B.; Jurasz, J.; Zhang, Y.; Varini, M.; Stridh, B.; Yan, J. Li-ion batteries for peak shaving, price arbitrage, and photovoltaic self-consumption in commercial buildings: A Monte Carlo Analysis. *Energy Convers. Manag.* **2021**, *234*, 113889. [CrossRef]
105. Miao, L.; Lv, Y.; Zhu, D.; Li, L.; Gan, L.; Liu, M. Recent advances in zinc-ion hybrid energy storage: Coloring high-power capacitors with battery-level energy. *Chin. Chem. Lett.* **2022**, *34*, 107784. [CrossRef]
106. Dong, L.; Yang, W.; Yang, W.; Li, Y.; Wu, W.; Wang, G. Multivalent metal ion hybrid capacitors: A review with a focus on zinc-ion hybrid capacitors. *J. Mater. Chem. A* **2019**, *7*, 13810–13832. [CrossRef]

107. Durmus, Y.E.; Zhang, H.; Baakes, F.; Desmaizieres, G.; Hayun, H.; Yang, L.; Kolek, M.; Küpers, V.; Janek, J.; Mandler, D.; et al. Side by Side Battery Technologies with Lithium-Ion Based Batteries. *Adv. Energy Mater.* **2020**, *10*, 2000089. [[CrossRef](#)]
108. Toussaint, G.; Stevens, P.; Akrou, L.; Rouget, R.; Fourgeot, F. Development of a Rechargeable Zinc-Air Battery. *ECS Trans.* **2010**, *28*, 25–34. [[CrossRef](#)]
109. Chen, M.; Liu, Q.; Wang, S.-W.; Wang, E.; Guo, X.; Chou, S.-L. High-Abundance and Low-Cost Metal-Based Cathode Materials for Sodium-Ion Batteries: Problems, Progress, and Key Technologies. *Adv. Energy Mater.* **2019**, *9*, 1803609. [[CrossRef](#)]
110. Deng, Y.-P.; Liang, R.; Jiang, G.; Jiang, Y.; Yu, A.; Chen, Z. The Current State of Aqueous Zn-Based Rechargeable Batteries. *ACS Energy Lett.* **2020**, *5*, 1665–1675. [[CrossRef](#)]
111. Vereinte Nationen. *Globally Harmonized System of Classification and Labelling of Chemicals (GHS)*; United Nations: New York, NY, USA, 2021; ISBN 9789211172522.
112. Liu, Y.; Hu, J.; Lu, Q.; Hantusch, M.; Zhang, H.; Qu, Z.; Tang, H.; Dong, H.; Schmidt, O.G.; Holze, R.; et al. Highly enhanced reversibility of a Zn anode by in-situ texturing. *Energy Storage Mater.* **2022**, *47*, 98–104. [[CrossRef](#)]
113. Dürena, R.; Zukuls, A.; Vanags, M.; Šutka, A. How to increase the potential of aqueous Zn-MnO<sub>2</sub> batteries: The effect of pH gradient electrolyte. *Electrochim. Acta* **2022**, *434*, 141275. [[CrossRef](#)]
114. Yadav, G.G.; Turney, D.; Huang, J.; Wei, X.; Banerjee, S. Breaking the 2 V Barrier in Aqueous Zinc Chemistry: Creating 2.45 and 2.8 V MnO<sub>2</sub>–Zn Aqueous Batteries. *ACS Energy Lett.* **2019**, *4*, 2144–2146. [[CrossRef](#)]
115. Shen, Z.; Tang, Z.; Li, C.; Luo, L.; Pu, J.; Wen, Z.; Liu, Y.; Ji, Y.; Xie, J.; Wang, L.; et al. Precise Proton Redistribution for Two-Electron Redox in Aqueous Zinc/Manganese Dioxide Batteries. *Adv. Energy Mater.* **2021**, *11*, 2170162. [[CrossRef](#)]
116. Cui, Y.-F.; Zhuang, Z.-B.; Xie, Z.-L.; Cao, R.-F.; Hao, Q.; Zhang, N.; Liu, W.-Q.; Zhu, Y.-H.; Huang, G. High-Energy and Long-Lived Zn-MnO<sub>2</sub> Battery Enabled by a Hydrophobic-Ion-Conducting Membrane. *ACS Nano* **2022**, *16*, 20730–20738. [[CrossRef](#)]
117. Zhong, C.; Liu, B.; Ding, J.; Liu, X.; Zhong, Y.; Li, Y.; Sun, C.; Han, X.; Deng, Y.; Zhao, N.; et al. Decoupling electrolytes towards stable and high-energy rechargeable aqueous zinc–manganese dioxide batteries. *Nat. Energy* **2020**, *5*, 440–449. [[CrossRef](#)]
118. Han, B.; Risch, M.; Belden, S.; Lee, S.; Bayer, D.; Mutoro, E.; Shao-Horn, Y. Screening Oxide Support Materials for OER Catalysts in Acid. *J. Electrochem. Soc.* **2018**, *165*, F813–F820. [[CrossRef](#)]
119. de Guzman, R.N.; Awaluddin, A.; Shen, Y.-F.; Tian, Z.R.; Suib, S.L.; Ching, S.; O’Young, C.-L. Electrical Resistivity Measurements on Manganese Oxides with Layer and Tunnel Structures: Birnessites, Todorokites, and Cryptomelanes. *Chem. Mater.* **1995**, *7*, 1286–1292. [[CrossRef](#)]
120. Shen, Z.; Liu, Y.; Luo, L.; Pu, J.; Ji, Y.; Xie, J.; Li, L.; Li, C.; Yao, Y.; Hong, G. Interface Engineering of Aqueous Zinc/Manganese Dioxide Batteries with High Areal Capacity and Energy Density. *Small* **2022**, *18*, e2204683. [[CrossRef](#)] [[PubMed](#)]
121. Ruan, P.; Liang, S.; Lu, B.; Fan, H.J.; Zhou, J. Design Strategies for High-Energy-Density Aqueous Zinc Batteries. *Angew. Chem. Int. Ed.* **2022**, *61*, e202200598. [[CrossRef](#)]
122. Chen, W.; Li, G.; Pei, A.; Li, Y.; Liao, L.; Wang, H.; Wan, J.; Liang, Z.; Chen, G.; Zhang, H.; et al. A manganese–hydrogen battery with potential for grid-scale energy storage. *Nat. Energy* **2018**, *3*, 428–435. [[CrossRef](#)]
123. Ronen, R.; Atlas, I.; Suss, M.E. Theory of Flow Batteries with Fast Homogeneous Chemical Reactions. *J. Electrochem. Soc.* **2018**, *165*, A3820–A3827. [[CrossRef](#)]
124. Rolle, M.; Sprocaci, R.; Masi, M.; Jin, B.; Muniruzzaman, M. Nernst-Planck-based Description of Transport, Coulombic Interactions, and Geochemical Reactions in Porous Media: Modeling Approach and Benchmark Experiments. *Water Resour. Res.* **2018**, *54*, 3176–3195. [[CrossRef](#)]
125. Singh, M.R.; Papadantonakis, K.; Xiang, C.; Lewis, N.S. An electrochemical engineering assessment of the operational conditions and constraints for solar-driven water-splitting systems at near-neutral pH. *Energy Environ. Sci.* **2015**, *8*, 2760–2767. [[CrossRef](#)]
126. Clark, S.; Latz, A.; Horstmann, B. Rational Development of Neutral Aqueous Electrolytes for Zinc-Air Batteries. *ChemSusChem* **2017**, *10*, 4735–4747. [[CrossRef](#)]
127. Saaltink, M.W.; Carrera, J.; Ayora, C. On the behavior of approaches to simulate reactive transport. *J. Contam. Hydrol.* **2001**, *48*, 213–235. [[CrossRef](#)] [[PubMed](#)]
128. Tran, M.-K.; DaCosta, A.; Mevawalla, A.; Panchal, S.; Fowler, M. Comparative Study of Equivalent Circuit Models Performance in Four Common Lithium-Ion Batteries: LFP, NMC, LMO, NCA. *Batteries* **2021**, *7*, 51. [[CrossRef](#)]
129. Tran, M.-K.; Mathew, M.; Janhunen, S.; Panchal, S.; Raahemifar, K.; Fraser, R.; Fowler, M. A comprehensive equivalent circuit model for lithium-ion batteries, incorporating the effects of state of health, state of charge, and temperature on model parameters. *J. Energy Storage* **2021**, *43*, 103252. [[CrossRef](#)]
130. Lai, X.; Wang, S.; Ma, S.; Xie, J.; Zheng, Y. Parameter sensitivity analysis and simplification of equivalent circuit model for the state of charge of lithium-ion batteries. *Electrochim. Acta* **2020**, *330*, 135239. [[CrossRef](#)]
131. Farmann, A.; Sauer, D.U. Comparative study of reduced order equivalent circuit models for on-board state-of-available-power prediction of lithium-ion batteries in electric vehicles. *Appl. Energy* **2018**, *225*, 1102–1122. [[CrossRef](#)]
132. Bischoff, C. Herstellung und Charakterisierung von Zink-Ionen-Batteriezellen für Stationäre Anwendungen. Ph.D. Thesis, Albert-Ludwigs-Universität Freiburg im Breisgau, Freiburg, Germany, 2022.